Mixing and Residence Time Distribution Studies in Microchannels with Floor Herringbone Structures

Alberto Cantu-Perez, Suet Ping Kee and Asterios Gavriilidis*
University College London, Department of Chemical Engineering, Torrington Place, London, WC1E 7JE, UK.
*Corresponding author: a.gavriilidis@ucl.ac.uk

Abstract: The mixing characteristics and residence time distribution (RTD) of a microchannel with floor staggered herringbone structures have been investigated numerically with COMSOL Multiphysics 3.3 and particle tracking algorithms that incorporate diffusion via a random walk approach. The RTD simulations were compared with experimental data. Mixing length was obtained for different mixing ratios and inlet stream arrangement. For all cases, it was found that placing one of the inlet streams in the centre gave lower mixing lengths. Residence time distributions were obtained for different operational and geometrical parameters. It was found that for low Peclet numbers the use of herringbone structures has little impact on the RTD. However, at higher Peclet numbers the herringbone channels have a narrower RTD than a rectangular channel. This behavior allows increasing the characteristic channel dimensions or the flowrate without compromising its performance in terms of RTD.

Keywords: Residence time distributions, micromixing, microchannels.

1. Introduction

The use of miniaturised devices for applications in micro total analysis systems, lab-on-a-chip and chemical process technology is becoming increasingly widespread. Intensive research has been focused on microprocess technology due to its advantages compared to macroscopic equipment in terms of high heat and mass transfer. Conversion and selectivity in chemical reactions is strongly dependent on the degree of mixing and the residence time distribution (RTD) of the reactor. Usually a narrow RTD is preferred as this would in principle be beneficial for both conversion and selectivity. The fluid flow in microchannels is laminar, thus mixing relies only in diffusion mechanisms rather than turbulence as in most macroscopic applications. A dimensionless number that compares convection over diffusion processes is the Peclet number, *Pe*:

$$Pe = \frac{U\,d}{D} \qquad (1)$$

where U is the fluid velocity, d is the characteristic length of the channel and D is diffusivity. For high Peclet numbers (typical for liquid flows) convection dominates the mixing process *[1]* and the mixing length in a microchannel would be too long. Furthermore the RTD in plain microchannels with high Peclet numbers is characterised by an asymmetric profile which may negatively impact conversion and selectivity of a chemical reaction. Staggered Herringbone Micromixers (SHM) increase the interfacial area and decrease the diffusion path achieving complete mixing in a much lower distance than a plain channel relying only on diffusion *[2]*. Moreover, they help in narrowing the RTD.

Although several investigations have been presented regarding the behavior of the SHM under different conditions *[3-6]*, they have been performed with a flow ratio 1:1. However, in general the flow ratio may be different. In this study we consider the effects of three different mixing ratios (1:1, 1:5 and 1:10) in the performance of the SHM and its impact on the necessary mixing length, each with two injection locations of the minor stream: at the centre or the side of the channel. Also the RTD of a microchannel with floor staggered herringbone structures is compared to that of a plain microchannel. The possibility of larger channels with staggered herringbone structures that behave similarly to plain microchannels is also considered. This has significant implications for some of the common problems related to microreaction technology like high pressure drop and channel blockage.

3. Geometry

The mixer geometry presented on this section is based on the one presented by Stroock et al. *[2]*, with asymmetric herringbones on the floor of the channel, which creates a pair of counter-rotating vortices. The degree of asymmetry *p* is characterised by the fraction of channel width occupied by the wide arm of the herringbones (*p=2/3* for the staggered herringbone channel). The asymmetry of the herringbone switches its position every half cycle allowing to change the position of the vortices, creating a flow pattern similar to the blinking vortex model proposed by Aref *[7]*. The mixer consists of several mixing cycles where each cycle is composed of two sets of grooves with the centre of the asymmetry alternated (Figure 1). For mixing considerations the channel width is 200 μm and the channel height is 85 μm. The grooves are placed at an angle θ=45° with respect to the axial direction. The depth of the grooves is 30.6 μm, and the groove wave vector, *q* is $2\pi/100$ μm^{-1}. The fluid properties for mixing simulations were the same as the ones used by Stroock et al. *[2]* (density=1200kg/m^3, viscosity=0.067Pa.s). For RTD measurements apart from the staggered herringbone channel a symmetric herringbone (with *p*=1/2) and a rectangular channel were also considered. For the channels with herringbone structures the groove depth was 0.17mm, the groove width was 0.7mm and the ridge width was 0.3mm (measured along the axial direction). The widths of the channels were 2mm for all cases and their heights were 0.85, 0.81 and 0.71mm for the rectangular, symmetric and staggered herringbone channels respectively. The fluid properties for RTD simulations were those of water with density=1000 kg/m^3 and viscosity= 0.001Pa.s. The dimensions for the channels used for RTD theoretical studies are the same as those employed for experimental RTD investigations. Due to the repeating cycles, the velocity field in the axial direction can be assumed to be periodic and hence the velocity field in one cycle can be obtained and reused repeatedly for successive cycles. The direction of the flow is from left to right.

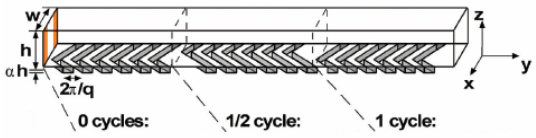

Figure 1. Geometry of the staggered herringbone micromixer *[2]*.

2. Use of COMSOL Multiphysics

The Navier-Stokes and the continuity equation for the conservation of mass, equations (2) and (3) respectively, are solved simultaneously with the fluid dynamics application in COMSOL Multiphysics 3.3.

$$\rho\frac{\partial v}{\partial t}-\nabla\cdot\left[\eta\left(\nabla v+(\nabla v)^{T}\right)\right]+\rho(v\cdot\nabla)v+\nabla p=0 \qquad (2)$$

$$\nabla\cdot v=0 \qquad (3)$$

where ρ is density, v is velocity field, η is dynamic viscosity, p is pressure, and t is time. The velocity field is solved using periodic boundary conditions so that the velocity at the outlet boundary is the same to the inlet one, with a constant flow rate throughout the channel. Additionally, non-slip boundary conditions are applied to all walls. A mesh consisting of 30,712 number of elements and 156,256 degrees of freedom is used to execute the simulations in Windows XP with Pentium IV 3.00 GHz CPU and 2 GB of RAM. The solution is exported to MATLAB and a particle tracking algorithm with a random walk type diffusion step obtains the position of the particles by solving equation (4) for a fixed time step. The positions of the particles are recorded and the procedure is repeated over a specified number of steps.

$$d\vec{x}=v\left(\vec{x}\right)dt+\sqrt{2Ddt}\,\xi \qquad (4)$$

where $\vec{x}$ is the vector with the positions of the particles. The code is set so that the velocity field obtained for the first cycle could be used over many mixing cycles. A standard fourth order Runge-Kutta method with fixed time steps is used to obtain the solution. For the mixing simulations only the convective part of the particle tracking code is used (first term in equation (4)) which is valid in the limit of negligible diffusion.

4. Methods

4.1 Mixing

Mixing is characterized by three different methods: nearest neighbor analysis*[4]*, stretching histories*[5]* and striation thickness reduction *[4]*. In the nearest neighbor analysis, the positions of the tracer particles after certain number of mixing cycles are compared with the positions of particles distributed uniformly throughout the cross section. By calculating the distances between the tracer particles and the particles in the uniform array a measure of percentage of mixing can be calculated by checking the percentage of particles that are already distributed uniformly. The stretching histories method needs first the calculation of the stretching of a vector l associated to every particle.

$$\frac{d(l)}{dt} = (\nabla U)^T . l \qquad l_{t=0} = l_0 \tag{5}$$

The total accumulated stretch is defined as:

$$\lambda = \frac{|l|}{|l_0|} \tag{6}$$

and the specific stretch is obtained from:

$$a = \lim_{t\to\infty}\left[\frac{1}{t}\ln(\lambda_m)\right] \tag{7}$$

finally the required time for mixing is obtained from *[5, 8]*:

$$t = \frac{\ln\left(\frac{(s(0))^2 2a}{D} + 1\right)}{2a} \tag{8}$$

The average striation thickness at the end of various cycles is measured by identifying patterns of striations in the particles. At the end of every cycle a snapshot of the plane z-x and a sample of 5 μm height of the whole cross-section are taken, the positions of the particles are recorded within this small part of the mixer like shown in Figure 2. The thickness of the striations are measured by identifying the initial and final particle of the striation, if the particles are separated within a distance of 2.5 μm then is considered that they belong to the same striation. If the flow is chaotic then the striation thickness should decrease exponentially. The specific stretch of equation (7) is related to the striation thickness evolution according to equation (9)*[8]*:

$$s(t) = \frac{s(0)}{\lambda} = \frac{s(0)}{e^{(at)}} = s(0)e^{(-at)} \tag{9}$$

a graph of striation thickness versus time can be fitted to an exponential function with parameter *a*, and mixing time can be calculated again with equation (8).

a) b)

Figure 2. a) Particles at the end of 3rd cycle at a height between 40 and 45 mm, b) Particles at the end of 3rd cycle on the whole cross-section.

4.2 Residence time distribution

Numerical RTDs are obtained by recording the number of particles arriving at the channel exit, N_i, as a function of time interval, $\Delta t_i = t_{i+1} - t_i$, with equation (10):

$$E(t_i) = \frac{N_i}{\sum_{i=1}^{n} N_i \Delta t_i} \tag{10}$$

The RTD in dimensionless form is obtained

from:

$$E(\theta) = t_m E(t_i) \tag{11}$$

where t_m is the mean residence time. The variance of the distribution can be calculated as follows:

$$\sigma^2 = \frac{\sum_{i=1}^{n}(t_i - t_m)^2 E(t_i)\Delta t}{\sum_{i=1}^{n} E(t_i)\Delta t} \tag{12}$$

which in dimensionless form changes to:

$$\sigma_\theta^2 = \frac{\sigma^2}{t_m^2} \qquad (13)$$

Experimental RTDs were obtained by injecting an inert tracer into the channels and recording its concentration at the outlet with a LED-photodiode array developed for this purpose. The experimental channels were fabricated on a plate of PMMA (Polymethylmethacrylate) (RS-components),8cm x 8cm x 3mm by an engraving machine (Roland EGX-400). The engraved PMMA plates were cleaned in an ultrasonic bath for 20 minutes with Decon 90 and dried with an air gun. To produce closed channels the plate was clamped along with a top PMMA plate with feed-through holes in a stainless steel jig and placed in an oven (Lenton WF30) for 10 minutes at 110°C (close to the PMMA softening temperature) for bonding. An HPLC pump (Waters 510) was used for feeding deionized water to the chip (flowrates 0.5 and 1 ml/min). The tracer pulse (Parker Blue dye) was introduced by a 6-port sample injection valve (Rheodyne) equipped with 5 µl sample loop and an internal position signal switch that indicates the time of injection. The piping among all components was Teflon 0.254mm ID. Tracer detection was performed by light absorption. Illumination was provided by two square LEDs (Kingbright L-1553IDT). To make sure that only light going through the desired channel area was collected black tape was used to mask the neighboring areas. To seal the system from ambient light it was placed in a dark box. The detection system was based on a linear diode array detector (TSL, 1401R-LF) which had 128 diodes each of dimensions 63.5 microns by 55.5 microns. Data from the sensor was collected using a National instruments PCI-6010 data acquisition card before being analysed and displayed on a computer using a program written in Labview. Every 100 ms the computer would average the previous two scans, calculate the absorbance for each diode and display the result. The absorbance of the tracer dye was found to be in accordance with the Beer-Lambert law.

5. Results and Discussion

5.1 Mixing

Mixing simulations have been compared with experimental data reported by Stroock et al. *[2]* . Figure 3 shows the evolution of mixing after 1 cycle for a mixing ratio of 1:1 with initial positions of the tracer on the right of the channel. The agreement between the graphs is good and the procedure to calculate mixing is considered to be valid.

a) b)

Figure 3. Comparison of mixing simulations with experimental data from Stroock et al. *[2]* after 1 mixing cycle. a) Comsol simulation, b) confocal micrograph.*[2]*

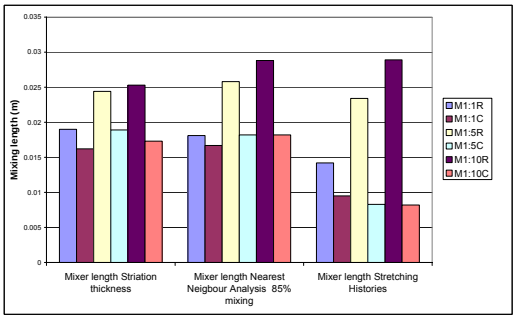

Figure 4. Mixing lengths obtained from three different methods for all mixing ratios and injection locations. The first part of the tag indicates the mixing ratio and last letter the injection location so that M1:1R indicates the results for mixing ratio 1:1 injected on the right side of the channel.

Mixing lengths were obtained with the three different methods described in section 4.1 for three mixing ratios (1:1, 1:5 and 1:10) and two different injection locations of the minor stream at the right or at the centre of the channel. The results are shown on figure 4. All three methods show that for all cases placing one of the fluids in the centre of the channel gives lower mixing lengths than when the fluid is on the right. The mixing length for a mixing ratio of 1:1 when one of the fluids is on the right of the channel (case

M1:1R) is between 1.4 and 1.9 cm this is in accordance to the experimental mixing length of 1.7 cm obtained by Stroock *et al. [2]*.

The fact that placing one of the fluids at the centre of the channel gives better mixing results is supported by the spatial distribution of stretching shown in Figure 5. The areas of highest stretching and therefore highest micromixing *[9]* are located on the sides of the channel. The grooves are responsible for transporting material from the centre to the sides of the channel ensuring that the particles sample the regions of highest stretching.

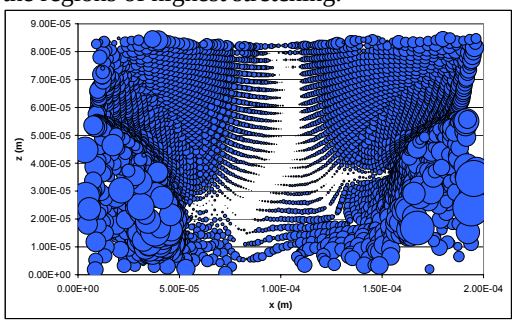

Figure 5. Relative stretching of the fluid elements. The sizes of the circles indicate the relative magnitude of the stretching.

5.2 Residence time distributions

Residence time distributions were obtained for a rectangular channel and channels with staggered and symmetrical herringbones. Figure 6 shows a comparison between RTDs obtained from experiments and from Comsol simulations for Pe~10^4. The agreement between experiments and simulations is shown to be good. The RTD for the rectangular channel is characterized by an early peak close to half the mean residence time followed by a long tail ($\sigma_\theta^2 = 0.223$), whereas for the channels with herringbone structures the distributions are narrower, $\sigma_\theta^2 = 0.049$ and $\sigma_\theta^2 = 0.064$ for the staggered and symmetrical herringbone respectively.

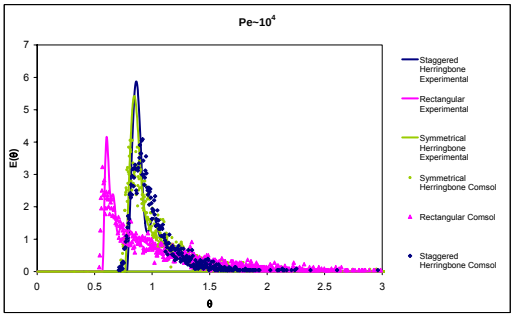

Figure 6. Dimensionless RTD obtained from experiments (solid lines) and simulations in Comsol (symbols) for channels with and without herringbone structures, at Pe~10^4.

Figure 7 shows that when the Peclet number is reduced to Pe~10^3 the channels with herringbone structures still have a narrower RTD evidenced by its lower variance $\sigma_\theta^2 = 0.029$, $\sigma_\theta^2 = 0.033$ for the staggered and symmetrical herringbone respectively than a rectangular channel $\sigma_\theta^2 = 0.069$, but the difference is not as great as in the case for Pe~10^4.

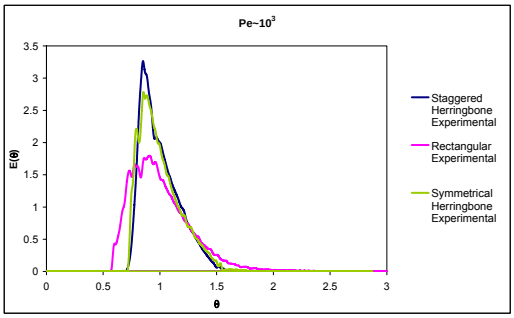

Figure 7. Dimensionless RTD obtained from experiments for channels with and without herringbone structures, at Pe~10^3.

On the other hand, as the Peclet number increases the RTD remains unchanged as shown on the RTDs obtained from simulations in Figure 8. This result has been pointed out recently by Vikhansky *[10]* who showed that for a chaotic flow the RTD is practically independent of Pe. Such behavior opens the possibility of increasing the velocity or the hydraulic diameter of the channels (increase Pe) without compromising its performance in terms of residence time distribution. This will help in solving some of the problems associated with microchannels like high pressure drop and susceptibility to clogging.

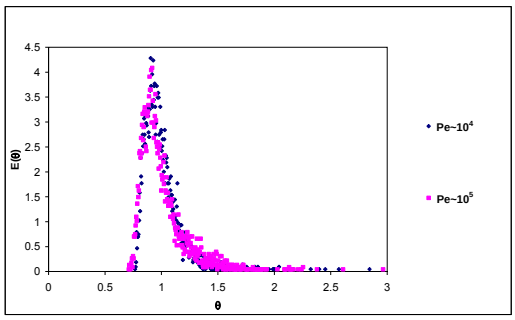

Figure 8. Dimensionless RTD obtained from simulations for channels with staggered herringbone structures, at Pe~10^4 and Pe~10^5.

A sensitivity analysis of the influence of the groove's geometrical parameters on the residence time distribution was carried out. The variances for all cases were calculated and compared to the reference case with 45° groove angle, 31 μm depth and 50 μm width and are shown in Table 1. At an angle of 30° and 60° the variances of the RTD are 0.392 and 0.0796 respectively, compared to 0.0617 of the reference case. The analysis on the groove depth shows that the RTD exhibits a higher variance at both low and high depths (15 and 60 μm respectively) than that of the reference case. The groove width has a significant impact on the RTD. Both for wider and narrower grooves the distribution is worsened with respect to the reference case. This analysis show that for all three parameters investigated, there must be an optimum value that lies within the lower and upper bounds of the variables. Judging from the values in table 1 the reference case is close to the optimum as this gave the lowest variance σ_θ^2=0.0617.

Table 1. Influence of groove geometrical parameters (angle, depth and width) on the variance of the RTD for a staggered herringbone channel.

Influence of angle	σ_θ^2=0.0654 θ=30°	σ_θ^2=0.0206 θ=45°	σ_θ^2=0.0796 θ=60°
Influence of depth	σ_θ^2=0.0852 d_g=15μm	σ_θ^2=0.0206 d_g=31μm	σ_θ^2=0.0194 d_g=60μm
Influence of width	σ_θ^2=0.1113 w_g=30μm	σ_θ^2=0.0206 w_g=50μm	σ_θ^2=0.0517 w_g=70μm

6. Conclusions

The mixing characteristics of the staggered herringbone channel were investigated via numerical simulations and particle tracking for different mixing ratios and inlet stream locations. For all mixing ratios it was found that placing one of the fluids in the centre of the channel gave lower mixing lengths than when it is on the side. The presence of high stretching zones on the sides of the channel and the transportation of material by the grooves to these locations are thought to be responsible of the enhanced mixing. Furthermore residence time distributions were obtained numerically and experimentally for channels with staggered and symmetrical herringbone structures and compared with a rectangular channel. The results show that for low Peclet numbers (Pe<10^3) the use of herringbone structures does not impact significantly the RTD. However, for high Pe the channels with herringbone structures maintain a narrow RTD, whereas the RTD for the rectangular channel is significantly worsened. This allows increasing the velocity or the hydraulic diameter of the channels (increase Pe) without deteriorating the residence time distribution.

7. Acknowledgements

ACP would like to thank the scholarship granted by the Mexican Council for Science and Technology (CONACyT-Mexico)

8. References

1. Nguyen, N. T.; Wu, Z. G. Micromixers - a review. *Journal of Micromechanics and Microengineering* **2005,** *15* (2), R1-R16.

2. Stroock, A. D.; Dertinger, S. K.; Ajdari, A.; Mezic, I.; Stone, H. A.; Whitesides, G. M. Chaotic mixer for microchannels. *Science* **2002,** *295* (5555), 647-651.

3. Aubin, J.; Fletcher, D. F.; Bertrand, J.; Xuereb, C. Characterization of the mixing quality in micromixers. *Chemical Engineering & Technology* **2003,** *26* (12), 1262-1270.

4. Aubin, J.; Fletcher, D. F.; Xuereb, C. Design of micromixers using CFD

modelling. *Chemical Engineering Science* **2005,** *60* (8-9), 2503-2516.

5. Kee, S. P.; Gavriilidis, A. Design and characterisation of the staggered herringbone mixer. *Chemical Engineering Journal* **2008,** *142* (1), 109-121.

6. Kang, T. G.; Kwon, T. H. Colored particle tracking method for mixing anlysis of chaotic micromixers. *Journal of Micromechanics and Microengineering* **2004,** *14* (7), 891-899.

7. Aref, H. Stirring by Chaotic Advection. *Journal of Fluid Mechanics* **1984,** *143* (JUN), 1-21.

8. Ottino, J. M.; Wiggins, S. Introduction: mixing in microfluidics. *Philosophical Transactions of the Royal Society of London Series A-Mathematical Physical and Engineering Sciences* **2004,** *362* (1818), 923-935.

9. Liu, M.; Peskin, R. L.; Muzzio, F. J.; Leong, C. W. Structure of the Stretching Field in Chaotic Cavity Flows. *Aiche Journal* **1994,** *40* (8), 1273-1286.

10. Vikhansky, A. Effect of diffusion on residence time distribution in chaotic channel flow. *Chemical Engineering Science* **2008,** *63* (7), 1866-1870.